Development of a quick and non-invasive measurement method for the extraction of the dispersion relation in CLT plates for the evaluation of the elastic parameters

Arved THIES[1]; Federica MORANDI[2]; Luca BARBARESI[2]; Massimo GARAI[2]; Jörn HÜBELT[1]; Niko KUMER[3]

[1] Hochschule Mittweida, Germany

[2] University of Bologna, Italy

[3] Stora Enso WP Bad St. Leonhard GmbH, Austria

ABSTRACT

This contribution discusses a quick and non-invasive method for the extraction of dispersion relations in CLT panels, with the aim of providing an estimate of the elastic parameters of the plates starting from the fitting of the experimental dispersion curve to the theoretical models.

Measurements were performed at the Stora Enso CLT mill on panels that have different thickness and orthotropic ratio. An instrumented hammer was used to excite the plate and accelerometers were used to acquire the impulse responses. Thanks to the reciprocity principle, the measurement points were kept fixed and the hitting point was moved; this allowed to reduce the measurement time and to decrease the number of accelerometers that must be attached.

The dispersion curves were evaluated using the phase shift method and the experimental results were fitted with the theoretical models for acoustically thick plates; finally, the elastic parameters were estimated.

The results give slightly low estimates of the Young's modulus and the shear modulus in the stiffer direction, while confirming the datasheet values in the less stiff direction, with deviations depending on the panel thickness. The precision of the hits is also analysed, while a reproducibility study is left for further developments.

Keywords: Cross Laminated Timber, Bending Wavenumbers, Structural Acoustics

1. INTRODUCTION

The CLT construction technique is widely used and can count on a distinct performance in building physics and structural features (1-3). Among the most relevant acoustic parameters that must be known for the characterization of a propagation medium, stand the velocities of longitudinal and bending waves, which are directly dependent on the elastic parameters of the material. Although these quantities can be accurately predicted for homogeneous materials, the anisotropic and inhomogeneous nature of wood complicates the estimate. Methods for the extraction of the elastic parameters by either vibrational testing (4) or by measurement of the dispersion relation (5) have been shown.

This paper presents a preliminary analysis of another quick and non-invasive method for the determination of the mechanical characteristics of CLT plates based upon the measurement of the dispersion relations. The work seeks a correlation between the vibro-acoustical characteristics of the CLT panels and the internal composition of the plies, in terms of numbers and thickness of the planks. To reach this goal, the velocities of longitudinal and bending waves were measured on different CLT panels characterized by: different total thickness, different number and thickness of the plies, different wood species and different surface qualities.

The dispersion relations are measured for eight panels in which all these parameters are varying and, through a fitting with theoretical models, the elastic constants of the panels are estimated. The final aim is to provide a comparison between the so-calculated values and the results of the structural

---

[1] athies1@hs-mittweida.de; huebelt@hs-mittweida.de

[2] federica.morandi6@unibo.it; luca.barbaresi@unibo.it; massimo.garai@unibo.it

[3] niko.kumer@storaenso.com

tests that are done for quality control purposes, and that imply a huge expense for laboratory tests.

Section 2 provides a brief presentation of the theoretical formulations for the dispersion relations of acoustically thick plates in contrast to the thin plate theory. Furthermore, the phase shift method which was used for the evaluation of the dispersion images is described.

Section 3 describes the measurement setup, the panels tested and the process used to extract the elastic parameters from the dispersion relations. Section 4 discusses the results of the comparison in terms of the Young's modulus E and the shear modulus G and provides an estimate on the uncertainty of the results calculated with the proposed method. Finally, the conclusion discusses the advantages and the limitations of the proposed approach and discusses potential improvements of the method.

2. BACKGROUND

2.1 Acoustically thick plates

The dispersion relation for bending waves in acoustically thin plates is well known and given in Eq. (1), where E is the Young's modulus, I the second moment of area, μ the Poisson ratio and m'' the surface mass of the plate. This equation is based on the Kirchhoff model of the thin plate and thus only holds under the assumption that shear forces are negligible.

$$c_{B,K} = \sqrt[4]{\frac{EI}{(1-\mu^2)m''}}\sqrt{\omega} \tag{1}$$

The most common model for thick plates is the Mindlin model (6), which takes shear forces into account. The dispersion relation for the bending waves according to Mindlin is given in an implicit formulation by Eq. (2). As a result of taking shearing forces into account, the maximum bending wave velocity c_S is limited by the non-dispersive shearing wave velocity which is given in Eq. (3), where G is the shear modulus and ρ the density. The longitudinal wave velocity c_L is given in Eq. (4), while the coefficient T, which takes the non-uniformity of the shear stress into account, is given in Eq. (5). The bending wavenumber $k_{B,K}$ which is used for the calculation, can be derived from Eq. (1).

$$\left(1 - \frac{c_{B,M}^2}{T^2 c_S^2}\right)\left(\frac{c_L^2}{c_{B,M}^2} - 1\right) = \frac{12}{h^2 k_{B,K}^2} \tag{2}$$

$$c_S = \sqrt{G/\rho}; \; c_L = \sqrt{E/\rho} \tag{3); (4}$$

$$T = \frac{0.87 + 1.12\mu}{1 + \mu} \tag{5}$$

A simplified model for the dispersion relation was presented by Rindel (7). It is based on the idea, that for low frequencies the bending wave velocity shows asymptotical behaviour towards the thin plate model, while for high frequencies it is asymptotic towards the shearing wave velocity. In this case the effective bending wave velocity is given by Eq. (6). For identical elastic parameters the difference between the models by Rindel and Mindlin is insignificant.

$$c_{B,eff} = \left[\frac{1}{c_{B,K}^3} + \frac{1}{c_S^3}\right]^{-1/3} \tag{6}$$

2.2 Phase shift method

An efficient method to measure the dispersion relations is a multichannel analysis. From this, the dispersion images can be directly computed by a wavefield transformation that will be referred to as the *phase shift method* in this paper.

The phase shift method is elaborately described and analysed by Park et. al. (8). It is based on transforming the recorded wavefield $U(x,t)$ from the space and time domains to the space and frequency domains to obtain $U(x,\omega)$. Now the wavefield can be expressed as the product of the amplitude spectrum $A(x,\omega)$ and the phase spectrum $P(x,\omega)$ which contains the information about the dispersion characteristics. By applying another integral transformation, the dispersion image $V(\omega,\phi)$ is obtained as shown in Eq. (7).

$$V(\omega, \phi) = \int e^{-j(\Phi - \phi)x} \frac{A(x, \omega)}{|A(x, \omega)|} dx \qquad (7)$$

For every frequency, V will have a maximum if Eq. (8) holds, i.e. if the measured bending wave velocity is employed. In case of orthotropic materials, the process must be performed in the two major directions.

$$\phi = \Phi = \omega/c_B \qquad (8)$$

The phase shift method is most commonly applied in geophysics and used for the measurement of the dispersion characteristics of surface waves (9). In acoustics similar methods have been applied and are best known as inhomogeneous wave correlation method or spatial Fourier transform (10).

3. MEASUREMENT SETUP

3.1 Testing configurations and procedure

Table 1 - Description of the panels tested.

Panel	Thickness [mm]	Layer composition	E_{major} [MPa]	E_{minor} [MPa]	$f_{c,major}$ [Hz]	$f_{c,minor}$ [Hz]	Orthotropic factor
1	180	40-30-40-30-40	10914	2086	73	167	5.2
2	180	40-30-40-30-40	10914	2086	73	167	5.2
3	120	40-40-40	12519	481	102	520	26.0
4	220	60-30-40-30-60	11857	1143	57	184	10.4
5	100	30-40-30	12168	832	124	475	14.6
6	100	30-40-30	12168	832	124	475	14.6
7	160	40-20-40-20-40	11578	1422	80	227	8.1
8	140	40-20-20-20-40	12015	985	89	312	12.2

In total, eight different CLT-panels of varying specifications and overall dimensions were tested. The characteristics of the different panels are shown in Table 1. Additional differences between the panels were the surface quality, which influences the moisture content of the wood and the wood species, which was spruce or pine with densities of 470 and 500 kg/m^3 respectively.

All panels were tested directly as they came out of the production line, before they were loaded for shipping. To ensure comparable boundary conditions, all panels were simply supported on two edges by two beams with cross sections of 9x9 cm. Two additional layers of expanded EPDM rubber were used for decoupling between the panel and the support. Since all CLT panels are made from an odd number of layers of orthogonal planks, they are inherently orthotropic. The stiffer direction of the panels will be referred to as x-direction.
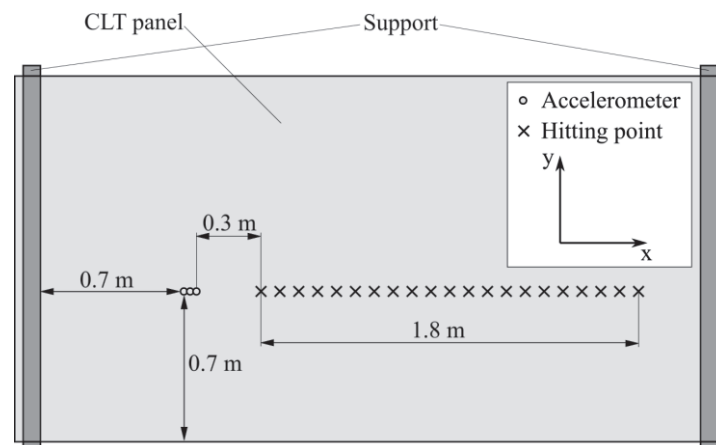

Figure 1 - Measurement setup for the bending wave velocity in x-direction.

The measurement setup for the multichannel analysis is shown in Figure 1. In total, only four channels were recorded for the measurement: one instrumented hammer and three accelerometers. All channels were recorded through a signal conditioner (PCB 482C15) connected to an RME Fireface 802 soundcard running at 192 kHz. The data was recorded in MATLAB® with the help of the ITA-Toolbox (11). The accelerometers (PCB 352C33) were placed in a line with 3 cm between each other and fixed to the panels with wax. Their position was chosen with a sufficient distance to the boundaries, hence the influence of boundary conditions and reflections could be minimized. The instrumented hammer (APTech AU02) was equipped with a rubber tip, so no dents were made in the wood, and 21 hits were executed on a previously drawn grid as shown in Figure 1. In the case of particularly small panels, it was made sure, that the distance between the last hitting point and the boundary was at least 0.7 m because otherwise negative effects caused by reflections showed. By aligning the recorded data of each hit in the time domain, an equivalent to a 64-channel measurement was created.

From the measured data, the dispersion images were calculated using the phase shift method.
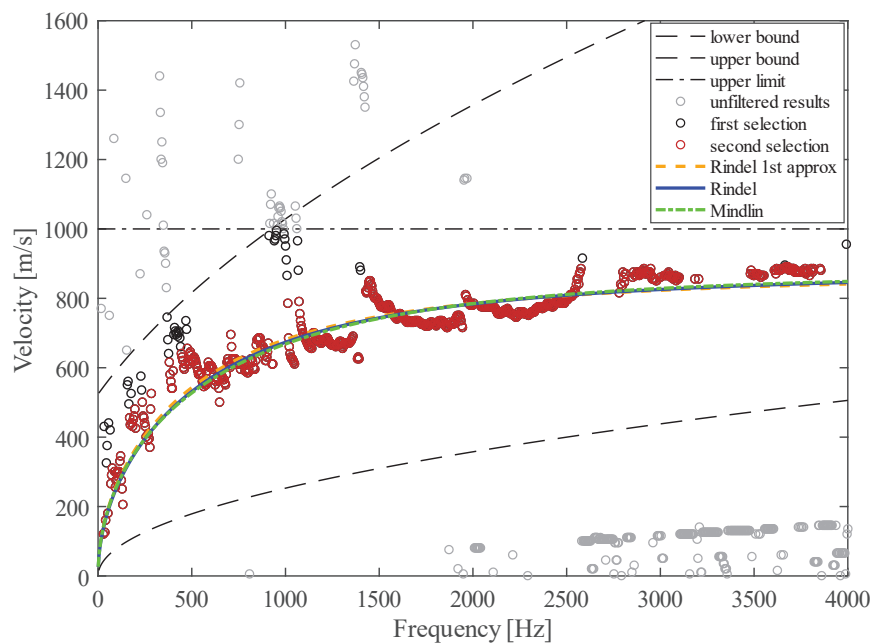
3.2   Intermediate data processing

Figure 2 - Dispersion relation measured for panel 8 (parallel to grain) and fitting with theoretical models.

Once the dispersion images were calculated, the experimental data was fitted with theoretical models to provide an estimate of the E and G moduli. Figure 2 shows the dispersion image for panel no. 8 in the x-direction. All circles represent the maximal value of the dispersion images for each frequency and thus the measured velocity for that frequency. It can be seen, that there are some spurious values and hence before the fitting, the data needed to be cleaned. The process is briefly summarized below.

1) A first selection of points was performed based on the fact, that c_B is limited by c_S. Because of that, a value sufficiently higher than the expected c_S value could be used as the upper limit above which all points got discarded. Further boundaries were chosen such that the influence of higher modes and aliasing effects could be minimized. The points discarded in step one are plotted in grey.
2) A preliminary fitting using Rindel's simplified model was performed.
3) All points that deviated past a certain threshold from the first fitting were discarded. These points are plotted in black.
4) Based on the second selection of points (red), the data was fitted with several models including Mindlin's model and Rindel's simplification. The Poisson ratio was kept fixed to 0.3.
5) Another fitting was performed with the same models and selection of points, only this time the Poisson ratio was included as a variable in the fitting.

4. DISCUSSION OF THE RESULTS

4.1 Comparison of *E* and *G*

All theoretical models used for the fitting of the data fit the measured dispersion images well, as can be seen for Rindel and Mindlin models in Figure 2. The measured values of the elastic parameters show differences between the models. The estimated values for the elastic parameters according to the models from Rindel and Mindlin of panel no. eight are shown in Table 2. For the two models the fitting was executed both with a Poisson ratio (μ) fixed to 0.3 as well as with μ as a parameter for the fitting. Rindel's simplified model showed spurious behaviour when μ was used as a variable, returning values out of the physically sensible range, while the dispersion of the elastic parameters for repeated measurements estimated with Mindlin's model with variable μ was bigger than with fixed μ. This might be due to not restraining μ during the fitting process and allowing different ratios among the different directions. Because of that, the values for the elastic parameters with variable μ were discarded and are not included in the further discussion.

The comparison of the remaining results shows a deviation between the repeated measurements of up to 20 %. This fact is discussed in section 4.2. All models deliver similar values with deviations smaller than 20 % for the elastic parameters with very few exceptions. Rindel's model generally delivers slightly lower values for both *E*- and *G*-modulus compared to Mindlin's. A graphical representation of this behaviour is given in Figure 3, while the tabular data for one panel is given in Table 2. Contrary to the variations in the elastic parameters, the estimates for the critical frequencies are very close together, both among the repeated measurements as well as between the different theoretical models.

Table 2 - Comparison of the measured elastic parameters for panel no. 8 from two repeated measurements.

Model	Rindel		Mindlin	
Measurement	1	2	1	2
E_{major} [MPa]	2914	3314	3310	3734
E_{minor} [MPa]	1046	923	1153	1055
G_{major} [MPa]	372	352	424	402
G_{minor} [MPa]	173	205	200	242
Orth. factor (*E*)	2,8	3,6	2,9	3,5
Orth. factor (*G*)	2,1	1,7	2,1	1,7
$f_{c,major}$ [Hz]	188	180	188	176
$f_{c,minor}$ [Hz]	344	352	356	356

Comparing the measured data to the values given in Table 1 shows greatly different results. In general, the tested panels can be divided into two different groups with a different behavior: the thick panels, consisting of five layers, and the thin panels, made from three layers of planks. For one panel of each group, a graphical comparison between the measured values and the datasheet values is given in Figure 3 in form of a radar chart.

In the group of the thick panels the measured values for E_{major} are generally much lower than the ones given in the datasheets. The measured values range from 60 to 70 % lower than the datasheet values, with higher deviations for higher orthotropic ratios. The measured values for E_{minor} on the other hand are very close to the datasheet values, averagely being around 10 % higher. However, there are deviations of up to ±15 % between the different tested panels, without any obvious correlation to the orthotropic factor.

Looking at the measured shear moduli in the group of the thick panels, there are huge deviations from the datasheet values. On average the measured G_{major} is almost one order of magnitude smaller than the datasheet value, again with larger differences for higher orthotropic factors. This difference is smaller for G_{minor} with a deviation of less than -50 % from the datasheet.
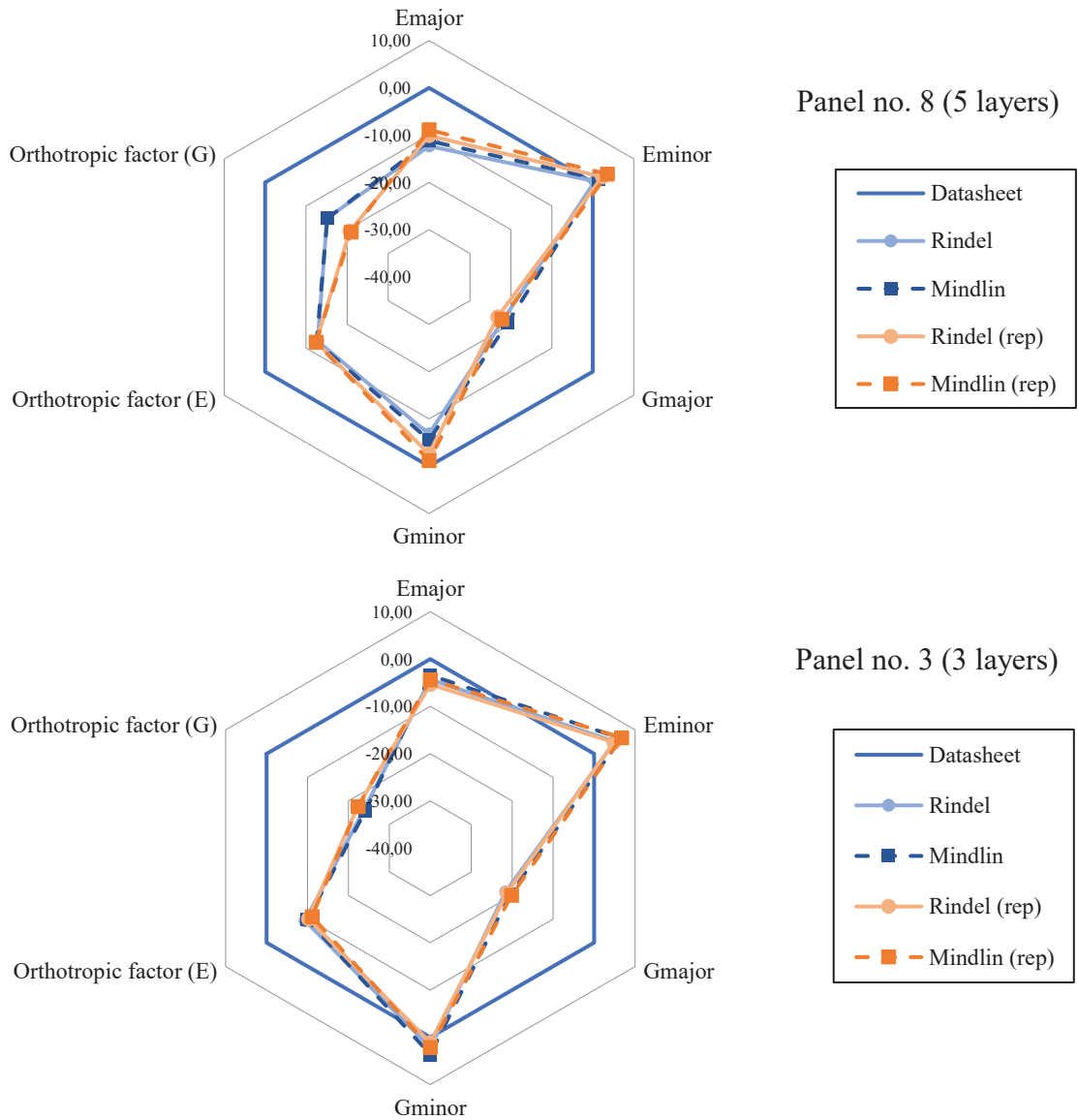
Figure 3 - Radar charts comparing the measured elastic parameters to the datasheet values for a 5-layer panel (top) and a 3-layer panel (bottom). For better comparability and legibility, the axes have been converted to a dB-scale relative to the datasheet value.

All this leads to a reduction of the measured orthotropic ratios down to between one quarter and one third of the datasheet values in terms of Young's moduli and an even bigger reduction to less than one quarter of the datasheet values in terms of shear moduli. The biggest dispersion in the data can be found in the measurements of G_{minor} and thus also in the orthotropic factor derived from the shear moduli. This is because the evaluation of the shear modulus is mainly influenced by the measured velocities for higher frequencies, which are particularly noisy in the y-direction.

In the group of the thin panels the general picture is similar, but there are some exceptions. While the measured E_{major} is still smaller than the datasheet values, the deviations are not as drastic with only -35 % for very high orthotropic factors. In terms of E_{minor} there are pronounced differences towards the thick panels. The measured values are up to 100 % higher than the datasheet values, again in case of the highest orthotropic factor.

Looking at G-moduli, this behaviour repeats in the less stiff direction with measured G_{minor} being higher than the datasheet value. In the stiffer direction the shear modulus is one order of magnitude smaller than the datasheet value, like with the thicker panels. This leads to an orthotropic factor of more than one order of magnitude smaller than the given value in terms of shear moduli. In terms of Young's moduli, the values are again around one third of the datasheet values. All in all, for the thinner three-layer panels the deviations between the theoretical models as well as among the repeated measurements are a little smaller, than for the thicker panels consisting of five layers.

One possible reason for the deviation of the measured elastic parameters from the datasheet values lies within the fact, that for the dynamic and non-invasive testing, the achievable strains are extremely small in comparison to the classical methods for the evaluation of the elastic parameters. Assuming that there is nonlinear behaviour in the stiffness of the wood, this is a possible explanation for the underestimation of the elastic parameters in the stiffer direction, which is especially apparent for the thicker panels.

4.2 Evaluation of the uncertainty of the measure and presentation of the hitting accuracy

As already shown in section 4.1, the values of the elastic parameters show deviations of up to 20 % between repeated measurements on the same panel. This limits the validity of the measured data, as well as the ability to measure small changes in the parameters.

One contribution to the uncertainty of the measurement can be found in the hitting accuracy. Since the instrumented hammer is operated by a person and the panel needs to be hit in several different points, there will be aberrations from the ideal hitting points. To investigate the amount of aberration, several measurements with a steel tip on the instrumented hammer were performed on a dummy panel. The steel tip left noticeable dents in the wood, such that the distance between the centre of the dent and the intended hitting point marked on the grid could be measured. This was done for both the longitudinal and the transverse deviations for 210 hitting points. The results are shown in Figure 4. The average absolute error is 1.9 mm and close to a normal distribution. Although less than two millimetres seem to be a small error this already represents almost seven percent of the distance between the accelerometers, making up a potential source for the noisy data and thus, the poor repeatability. Another potential source for noisy and dispersive data is the hitting strength. Especially for the thicker panels a compromise between exciting the panel properly and not leaving dents had to be made, with the priority in not leaving any dents in the panel.
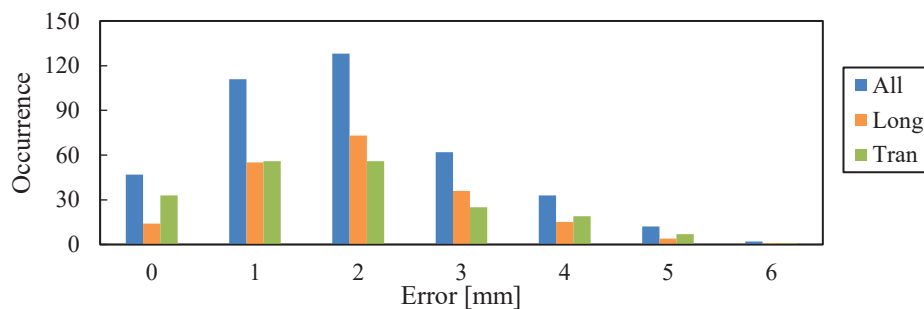

Figure 4 - Distribution of the aberrations from the actual hitting points in longitudinal, transverse and combined directions from the grid.

Another potential problem is the placement of the accelerometers, both in terms of noise in the data as well as the reproducibility. The accelerometers needed to be fixed to the panel for every measurement and although great care was taken to place them as accurately as possible, small variations in the sub millimetre range can not be ruled out. The problem with this error is that it is constant for all hitting points and not statistically evening out over the course of the measurement like the error regarding the hitting accuracy. Hence, even smallest deviations in the placement of the accelerometers might cause a significant variation in the results, especially in combination with the non-infinitesimal dimensions of the accelerometers and their inherent measurement uncertainty.

As noted in the beginning of this chapter, the data is especially noisy in the very low as well as in the upper frequency range of the measurement. In the low frequency range this is due to the pronounced modal behaviour of the CLT panels in that frequency range and the limited total length available for the measurement. Less than two meters of total distance were covered by the measurement and the dispersion image gets noticeably noisier as soon as the wavelengths start to get into that range. As a possible reason for the suboptimal behaviour for frequencies above 2 kHz aliasing was already mentioned. Checking with the measured data it can be seen that this should not be an issue since the shortest measured wavelengths were larger than 15 cm, while the spacing of the accelerometers with 3 cm is sufficiently smaller.

Summing up these factors leads to a noticeable uncertainty in the measurement of the dispersion images and thus the bending wave velocity. Additionally, the elastic parameters are extremely sensitive to small changes in measured velocity, for example the Young's modulus depends on the fourth power of c_B.

5. CONCLUDING REMARKS

A quick and non-inversive measurement method for the evaluation of the dispersion relation and thus, the elastic parameters of CLT-plates has been developed. By performing a multichannel analysis, that was optimised in terms of required channel count and measurement time, and processing it with the phase shift method, the dispersion images were obtained. From this, with the help of theoretical models for the acoustically thick plate, the elastic parameters of the tested panels were evaluated. The different models provide similar results, suggesting that the measurement method is valid. On the other hand, the measured values of the elastic parameters strongly deviate from the values given in the datasheet of the panels, although the deviations seem to follow a certain pattern. Generally, the measured values tend to be smaller than the calculated ones, which is especially apparent in the stiffer direction, leading to smaller orthotropic factors of the panels. In terms of the shear moduli this behaviour is even more pronounced, than for the Young's modulus.

As of now the accuracy and reproducibility of the proposed method is insufficient. Repeating measurements on the same panels showed deviations of up to 20 % for the elastic parameters, which renders the results of the measurements questionable. Small changes in the panel properties can not be measured reliably, while the big deviations between the repeated measurements make finding correlations between the orthotropic factors, the number of the panels and the elastic parameters difficult. Therefore, the collected data are not yet sufficient for finding improved models for the prediction of the acoustic behaviour of CLT-panels. On the upside, the measurements provide accurate results for the critical frequencies, with small deviations between different models and repeated measurements.

The main reasons for the deviations between the measurements seem to be the accuracy of the hitting with the instrumented hammer, as well as the placement of the accelerometers, which may be greatly improved on, by automating the process.

ACKNOWLEDGEMENTS

REFERENCES

1. Asdrubali F., Ferracuti B., Lombardi L., Guattari C., Evangelisti L., Grazieschi G. A review of structural, thermo-physical, acoustical and environmental properties of wooden materials for building applications. Building and Environment. 2017;114:307-322.
2. Caniato M., Bettarello F., Ferluga A., Marsich L., Schmid C. and Fausti P. Acoustic of lightweight timber buildings: a review. Renewable and sustainable Energy Reviews, 2017:80C: 585-596.
3. Caniato M., Bettarello F., Ferluga A., Marsich L., Schmid C. and Fausti P. Thermal and acoustic performance expectations on timber buildings. Building Acoustics, 2017:24(4):219-237.
4. Guan C., Zhang H., Wang X., Miao H., Zhou L., Liu F. Experimental and Theoretical Modal Analysis of Full-Sized Wood Composite Panels Supported on Four Nodes. Materials. 2017;10;
5. Santoni A., Schoenwald S., Van Damme B., Fausti P. Determination of the elastic and stiffness characteristics of cross-laminated timber plates from flexural wave velocity measurements. J. Sound Vib. 2017;400:387-401.
6. Graff K.F. Wave Motion in elastic solids. Dover Publications Inc. New York, 1975.
7. Rindel J.H. Dispersion and absorption of structure-borne sound in acoustically thick plates. Appl. Acoust. 1994;41:97-111.
8. Park CB, Miller RD, Xia J. Imaging dispersion curves of surface waves on multi-channel record. Society of Exploration Geophysicists 1998;10(1):1377-1380.
9. Park CB. Imaging Dispersion of MASW Data - Full vs. Selective Offset Scheme. Journal of Environmental and Engineering Geophysics 2011;16(1):13-23.
10. Van Damme B., Zemp A. Measuring Dispersion Curves for Bending Waves in Beams: A Comparison of Spatial Fourier Transform and Inhomogeneous Wave Correlation. Acta Acustica 2018; 103.
11. Berzborn M. et al. The ITA-Toolbox: An Open Source MATLAB Toolbox for Acoustic Measurements and Signal Processing. 43th Annual German Congress on Acoustics, Kiel, 2017.